Measurements of jet substructure and jet fragmentation using the ATLAS detector

Javier Llorente⋆, on behalf of the ATLAS Collaboration

Simon Fraser University. Burnaby, Canada

⋆ javier.llorente.merino@cern.ch

Proceedings for the XXVIII International Workshop on Deep-Inelastic Scattering and Related Subjects, Stony Brook University, New York, USA, 12-16 April 2021
doi:10.21468/SciPostPhysProc.8

Abstract

Measurements of the internal properties of jets at the LHC interaction scale allow QCD to be studied in a new energy regime. In this talk, we discuss recent measurements of jet substructure and jet fragmentation, which were performed using data collected by the ATLAS experiment at a centre-of-mass energy of $\sqrt{s} = 13$ TeV. The fragmentation properties of jets, such as the jet charge and summed fragmentation function, are measured using charged particles. A comprehensive suite of jet substructure observables is also measured for jets reconstructed with the soft-drop algorithm applied. In addition, a measurement of the Lund plane is performed using charged particles. All of the measurements are corrected for detector effects and are compared to the predictions of state-of-the-art Monte Carlo event generators.

Received 30-07-2021
Accepted 04-03-2022
Published 12-07-2022
doi:10.21468/SciPostPhysProc.8.080

1 Introduction

Measurements of jet substructure and jet fragmentation at the LHC are powerful tools to study QCD at the high-energy regime. These measurements provide sensitivity to basic aspects of the Monte Carlo simulation (MC) such as the parton shower (PS) and the hadronisation models, as well as allowing for tests of analytical predictions where soft-gluon resummation is implemented beyond leading logarithm. Experimentally, these measurements provide a useful insight to understanding the differences between quark- and gluon-initiated jets. These differences are key for reducing experimental uncertainties on the jet energy scale and resolution, which are typically dominant in physics analyses using final states containing jets such as, for instance, Higgs boson and top-quark decays. This work presents measurements of jet fragmentation using charged particles [1], substructure observables for jets groomed with the soft-drop algorithm [2] and a measurement of the Lund jet plane using charged particles [3]. All measurements use data from the ATLAS detector [4] at a centre-of-mass energy of $\sqrt{s} = 13$ TeV.

The measurements are compared to state-of-the-art MC predictions as well as to fixed-order theoretical predictions, and an interpretation in terms of the different properties of quark- and gluon-initiated jets is provided.

2 Measurement of jet fragmentation using charged particles

Jet fragmentation is a key aspect of QCD. Its measurements do not only provide an important insight on the modelling of hadron production within jets, but also a handle to understand the composition of jet production at the LHC. Quark- and gluon-initiated jets have different internal structure and fragmentation properties due to the larger colour factors of gluons. Since, for a given transverse momentum, quark jets tend to have a more forward rapidity distribution, the study of central and forward jets in dijet samples can help to disentangle both jet types.

The measurement of jet fragmentation using charged particles [1] is performed using dijet events reconstructed using the anti-k_t algorithm [5] with $R = 0.4$. Events with at least two jets with $p_{\mathrm{T}} > 60$ GeV and $|\eta| < 2.1$ are selected and, in order to ensure a good momentum balance between the two leading jets, the ratio of their transverse momenta is required to fulfil $p_{\mathrm{T}}^{(1)}/p_{\mathrm{T}}^{(2)} < 1.5$, where the indices 1 and 2 indicate the leading and subleading jets, respectively. Charged particles with $p_{\mathrm{T}} > 50$ MeV lying within $\Delta R = \sqrt{\Delta y^2 + \Delta\phi^2} = 0.4$ from the jet axis, where y is the rapidity and ϕ the azimuth, are selected and used to build the fragmentation observables. Two jet subsamples containing the more forward and more central jets from among the two leading jets in each event are selected, and their fragmentation properties are studied.

A set of variables sensitive to the fragmentation functions including the number of charged particles, the momentum fraction of charged particles with respect to the jet and the radial profile of the energy distribution of the charged particles, are measured for both the more central and the more forward jets. Since both subsamples are combinations of quark- and gluon-initiated jets in different proportions, they can be disentangled on average by solving the following system of linear equations:

$$\begin{cases} h_i^f = f_q^f h_i^q + (1 - f_q^f) h_i^g \\ h_i^c = f_q^c h_i^q + (1 - f_q^c) h_i^g. \end{cases} \tag{1}$$

The parameters h_i^f and h_i^c in Eq. 1 represent the values for the i-th bin of a given distribution for the more forward and more central jets, respectively, which are combinations of the quark and gluon values h_i^q and h_i^g. The coefficients f_q^x and f_g^x are the fractions of quarks and gluons in sample x (central or forward), respectively, and are obtained from MC simulation. Figure 1 shows the extracted quark and gluon distributions of the charged particle multiplicity for 1 TeV $< p_{\mathrm{T}} <$ 1.2 TeV, as well as the average value of the charged particle multiplicity as a function of the jet p_{T} for quark and gluon jets.

The average number of charged particles is compared to next-to-next-to-next-to-leading-order (NNNLO) predictions in QCD as well as to the MC predictions by PYTHIA [6] for both quark and gluon jets. For high values of the jet p_{T}, it is observed that both the NNNLO QCD and the LO+PS PYTHIA predictions largely overestimate the number of charged particles in gluon jets. The description of quark jets is more accurate, although it underestimates $\langle n_{\mathrm{ch}} \rangle$ at low p_{T} and overestimates it at high p_{T}.

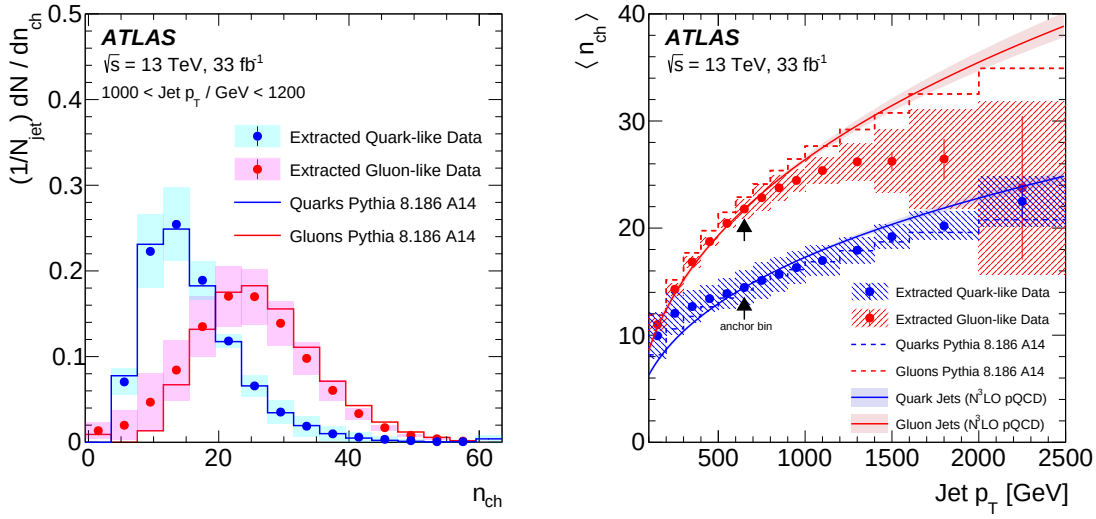

Figure 1: Distribution of the number of charged particles within the jet for quark and gluon jets with 1 TeV $< p_{\mathrm{T}} <$ 1.2 TeV (left). Average value of the number of charged particles $\langle n_{\mathrm{ch}} \rangle$ within quark and gluon jets as a function of the jet p_{T} (right) [1].

3 Measurement of soft-drop jet observables

Jet grooming techniques systematically remove soft and wide-angle radiation from the jet constituents. They are largely used at the LHC to remove contamination from sources different from the hard scattering, such as pileup or multiple parton interactions. The so-called soft drop algorithm [7] is one of these techniques which has been successfully used for the calculation of resummed theoretical predictions beyond leading-logarithm [8].

The measurement of soft-drop observables [2] is performed in dijet events, where both jets are clustered using the anti-k_t algorithm with $R = 0.8$ and are required to be well balanced ($p_{\mathrm{T}}^{(1)}/p_{\mathrm{T}}^{(2)} < 1.5$). The jet substructure inputs, either charged-particle tracks or calorimeter clusters are reclustered using the Cambridge-Aachen (C/A) algorithm [9] and the last step of the merging is undone, producing two subjets. The pair is evaluated using the soft-drop condition:

$$\frac{\min(p_{T1}, p_{T2})}{p_{T1} + p_{T2}} > z_{\mathrm{cut}} \left(\frac{\Delta R_{12}}{R} \right)^{\beta}. \tag{2}$$

If the condition in Eq. 2 does not hold, the subjet with the lowest p_{T} is removed and the procedure is repeated for the highest p_{T} subjet until the condition is satisfied.

Figure 2 shows the dimensionless mass parameter $\rho = \log\left(m^2/p_{\mathrm{T}}^2\right)$, where m is the groomed mass, compared to MC predictions by PYTHIA, SHERPA [10] and HERWIG++ [11], as well as with analytical predictions at fixed order with resummation implemented beyond leading logarithm. Among the parton shower MC predictions, PYTHIA gives the best description, while HERWIG++ fails to describe the data for low values of ρ. The analytical predictions agree well with the data in the regions where non-perturbative effects are small. Predictions without non-perturbative corrections applied fail to describe the data for low values of ρ, where these effects are important.

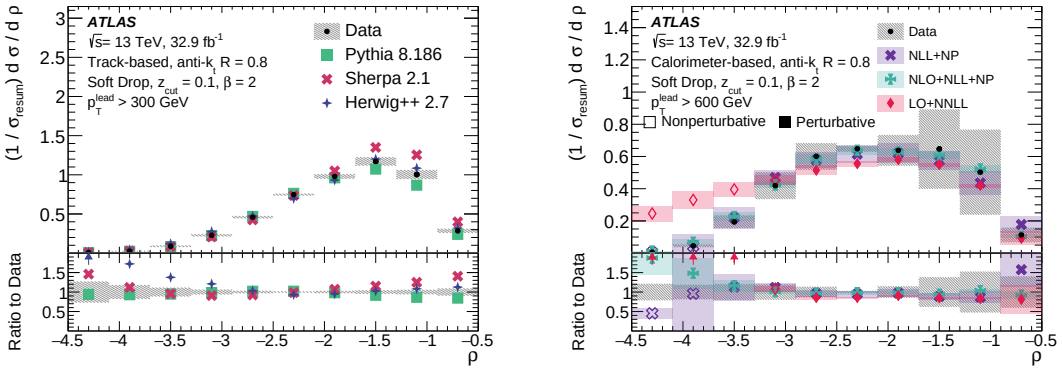

Figure 2: Distribution of the dimensionless mass parameter ρ for events with $p_{\mathrm{T}}^{\mathrm{lead}} > 300$ GeV (left), compared to MC predictions by PYTHIA, SHERPA and HERWIG++. Distribution of ρ for events with $p_{\mathrm{T}}^{\mathrm{lead}} > 600$ GeV (right) compared to analytical predictions. Jets entering both distributions are groomed using the soft-drop algorithm with $\beta = 2$ [2].

4 Measurement of the Lund jet plane using charged particles

The emission pattern of soft gluons with respect to hard partons can be characterized by the momentum fraction z of the emission with respect to the hard emitting parton and the opening angle θ between the gluon and the radiating parton. The so-called Lund plane [12] is a two-dimensional representation of these two observables, more precisely of $\ln(1/z)$ and $\ln(1/\theta)$. Recently, a jet-based analog to the Lund plane, obtained by declustering the jet history starting by the hardest subjet, has been proposed [13].

The measurement of the Lund jet plane [3] is performed in events with at least two jets clustered with the anti-k_t algorithm with $R = 0.4$, with a good momentum balance between the two leading jets ($p_{\mathrm{T}}^{(1)}/p_{\mathrm{T}}^{(2)} < 1.5$). All charged-particle tracks reconstructed within $\Delta R = 0.4$ from the jet axis are reclustered using the C/A algorithm and the clustering history is reversed and examined. For each splitting, the hardest subjet is designated as the 'core' while the softest subjet is designated as the 'emission', and the momentum fraction z and angular distance ΔR are defined as:

$$z = \frac{p_{\mathrm{T}}^{\mathrm{emission}}}{p_{\mathrm{T}}^{\mathrm{core}} + p_{\mathrm{T}}^{\mathrm{emission}}}; \qquad \Delta R^2 = (y_{\mathrm{core}} - y_{\mathrm{emission}})^2 + (\phi_{\mathrm{core}} - \phi_{\mathrm{emission}})^2.$$

The results are presented as a function of $\ln(R/\Delta R)$ and $\ln(1/z)$. The plane spanned by the two variables presents different regions, each of them being sensitive to a different physical effect. While the lower-left corner of the plane is sensitive to the hard, wide angle radiation pattern, the region close the main diagonal ($z\theta \simeq \Lambda_{\mathrm{QCD}}$) is sensitive to hadronisation effects. Other soft non-perturbative effects such as the underlying event or multiple parton interactions are represented in the region above the main diagonal.

Figure 3 shows the two-dimensional probability density as a function of both variables, as well as the distribution of $\ln(1/z)$ for $0.67 < \ln(R/\Delta R) < 1.00$, compared to MC predictions by PYTHIA, POWHEG+PYTHIA [14], SHERPA with two different hadronisation models (clusters and strings) and HERWIG 7 [15] with two different parton-shower algorithms, one angle-ordered and one dipole-based. None of these MC predictions describe the data well in all phase-space regions.

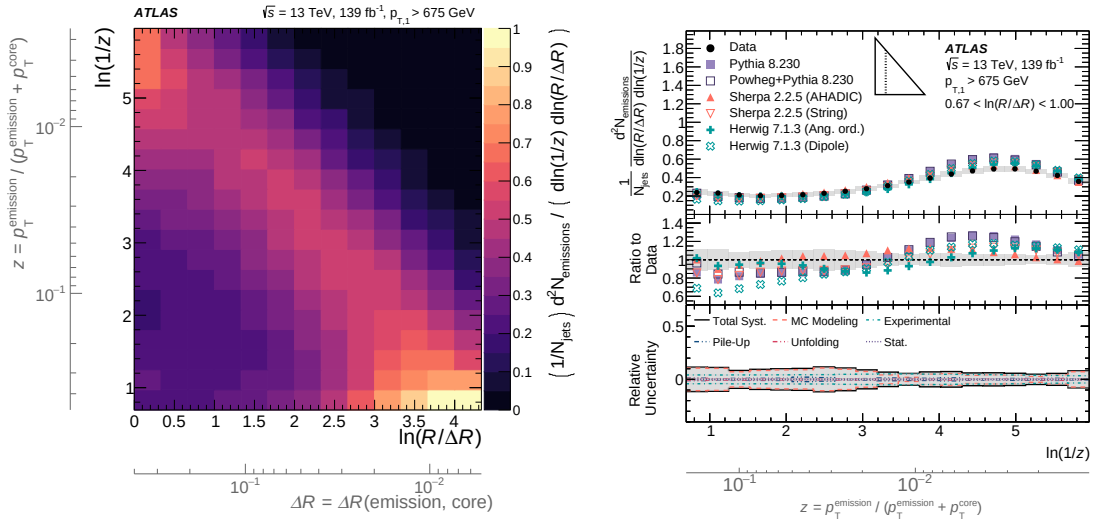

Figure 3: Two-dimensional probability density as a function of $\ln(R/\Delta R)$ and $\ln(1/z)$ (left) and distribution of $\ln(1/z)$ for $0.67 < \ln(R/\Delta R) < 1.00$ (right) [3].

5 Conclusions

Measurements of jet substructure and jet fragmentation in pp collisions at $\sqrt{s} = 13$ TeV using the ATLAS detector are presented. The results are compared to state-of-the-art Monte Carlo predictions, as well as to fixed-order analytical predictions with resummation implemented beyond the leading-logarithm approximation. In general, MC predictions would benefit of further tuning in order to describe the data fully in all regions of the phase space. Analytical predictions are in reasonable agreement with the data in the regions where non-perturbative effects are negligible, or once corrected for these effects.

The properties of quark- and gluon-initiated jets are extracted from the data for the analyses on jet fragmentation and soft-drop observables. This allows for a better understanding of the properties of both jet types and can help to constrain experimental uncertainties on jet energy scale and resolution.

References

[1] ATLAS Collaboration, *Properties of jet fragmentation using charged particles measured with the ATLAS detector in pp collisions at $\sqrt{s} = 13$ TeV*, Phys. Rev. D **100**, 052011 (2019), doi:10.1103/PhysRevD.100.052011.

[2] ATLAS Collaboration, *Measurement of soft-drop jet observables in pp collisions with the ATLAS detector at $\sqrt{s} = 13$ TeV*, Phys. Rev. D **101**, 052007 (2020), doi:10.1103/PhysRevD.101.052007.

[3] ATLAS Collaboration, *Measurement of the Lund Jet Plane Using Charged Particles in 13 TeV Proton-Proton Collisions with the ATLAS Detector*, Phys. Rev. Lett. **124**, 222002 (2020), doi:10.1103/PhysRevLett.124.222002.

[4] ATLAS Collaboration, *The ATLAS Experiment at the CERN Large Hadron Collider*, J. Inst. **3**, S08003 (2008), doi:10.1088/1748-0221/3/08/S08003.

[5] M. Cacciari, G. P. Salam and G. Soyez, *The anti-ktjet clustering algorithm*, J. High Energy Phys. **04**, 063 (2008), doi:10.1088/1126-6708/2008/04/063.

[6] T. Sjöstrand et al., *An introduction to PYTHIA 8.2*, Comput. Phys. Commun. **191**, 159 (2015), doi:10.1016/j.cpc.2015.01.024.

[7] A. J. Larkoski, S. Marzani, G. Soyez and J. Thaler, *Soft drop*, J. High Energy Phys. **05**, 146 (2014), doi:10.1007/JHEP05(2014)146.

[8] S. Marzani, L. Schunk and G. Soyez, *A study of jet mass distributions with grooming*, J. High Energy Phys. **07**, 132 (2017), doi:10.1007/JHEP07(2017)132.

[9] Yu. L. Dokshitzer, G. D. Leder, S. Moretti and B. R. Webber, *Better jet clustering algorithms*, J. High Energy Phys. **08**, 001 (1997), doi:10.1088/1126-6708/1997/08/001.

[10] T. Gleisberg, S. Höche, F. Krauss, M. Schönherr, S. Schumann, F. Siegert and J. Winter, *Event generation with SHERPA 1.1*, J. High Energy Phys. **02**, 007 (2009), doi:10.1088/1126-6708/2009/02/007.

[11] M. Bähr et al., *Herwig++ physics and manual*, Eur. Phys. J. C **58**, 639 (2008), doi:10.1140/epjc/s10052-008-0798-9.

[12] B. Andersson, G. Gustafson, L. Lönnblad and U. Pettersson, *Coherence effects in deep inelastic scattering*, Z. Phys. C - Particles and Fields **43**, 625 (1989), doi:10.1007/BF01550942.

[13] F. A. Dreyer, G. P. Salam and G. Soyez, *The Lund jet plane*, J. High Energy Phys. **12**, 064 (2018), doi:10.1007/JHEP12(2018)064.

[14] S. Alioli, P. Nason, C. Oleari and E. Re, *A general framework for implementing NLO calculations in shower Monte Carlo programs: the POWHEG BOX*, J. High Energy Phys. **06**, 043 (2010), doi:10.1007/JHEP06(2010)043.

[15] J. Bellm et al., *Herwig 7.1 Release Note*, arXiv:1705.06919.